ELSEVIER

Journal of Organometallic Chemistry 650 (2002) 249–257

Journal of Organometallic Chemistry

www.elsevier.com/locate/jorganchem

Investigation of the hydroformylation of ethylene in liquid carbon dioxide

Clement R. Yonker *, John C. Linehan

Fundamental Science Division, Pacific Northwest National Laboratory, Richland, WA 99352, USA

Received 16 July 2001; received in revised form 28 January 2002; accepted 29 January 2002

Abstract

In situ, high-pressure NMR was used to investigate the hydroformylation reaction of ethylene in liquid CO_2 using $Rh(CO)_2acac$ as the catalyst precursor and $(p\text{-}CF_3C_6H_4)_3P$, tris(*p*-trifluoromethylphenyl)phosphine, as the ligand under different thermodynamic conditions ($T = 10–23$ °C, $P_{CO} = P_{H_2} = 10–15$ bar, $P_{C_2H_4} = 10–15$ bar, $P_{CO_2} = 207$ bar). ^{1}H-NMR was used to monitor the reaction progress of the hydroformylation of ethylene with a rhodium catalyst under select conditions of temperature and CO_2 solvent pressure. Potential resting states of the rhodium catalyst were investigated by $^{31}P\{^1H\}$-NMR. This is the first description of a rhodium catalyzed hydroformylation reaction in liquid CO_2 monitored in situ by high pressure NMR.

Keywords: High pressure NMR; Carbon dioxide; Hydroformylation; Rhodium; Ethylene

1. Introduction

Supercritical fluids, as solvents for homogeneous catalytic reactions, have gained more attention over the past 10 years. Numerous groups have focused on the use of supercritical CO_2 as a solvent for hydrogenation, [1–5] carbon–carbon bond formation, [6,7] hydroformylation, [8–17] and olefin metathesis [18]. Supercritical CO_2 has some advantages over standard solvents, which include the ability to control solvent effects through changes in pressure and temperature, and high diffusivity/low viscosity. In addition, the high solubility of gases, in particular H_2, make supercritical CO_2 an attractive solvent. CO_2 has also been touted as an environmentally benign solvent for separations, extractions and chemical synthesis. A disadvantage of using CO_2 as a reaction solvent is the limited solubility of ligands and transition metal–phosphine complexes. Leitner et al. [13,14] and Palo and Erkey, [17] among others, have investigated the catalytic behavior of rhodium catalysts synthesized using 'CO_2-philic' fluoro-substituted phosphines which have enhanced solubility in CO_2. These hydroformylation investigations in supercritical CO_2 have all involved the use of a liquid alkene substrate for the experimental studies. This limits the reaction temperature range to ~31 °C and above for a single fluid homogeneous phase. The current experimental effort involves the use of gaseous ethylene dissolved in CO_2, which allows the direct determination of lower temperature reaction rates and the species present in liquid CO_2. Another factor limiting experimental study of supercritical fluid reaction systems involves the use of high-pressure spectroscopic techniques. Most experimental studies of hydroformylation reactions in both liquid and supercritical fluid solvents have involved the use of high-pressure FTIR spectroscopy, due to the high sensitivity of the technique. NMR can give quite detailed molecular information regarding the structure of reactants, products and intermediates, but this can be restricted by the need for concentrations in the range of 10–100 mM. Therefore, in situ high-pressure NMR studies of hydroformylation reactions have been limited. Rathke et al. [8–10] have focused on cobalt-carbonyl catalysts, studying the linear to branched ratio of the product aldehyde under supercritical conditions using their toroid coil high-pressure NMR cell. Leitner et al. [19] have used a single-crystal

* Corresponding author. Tel.: +1-509-372-4748; fax: +1-509-375-6660.

E-mail address: clem.yonker@pnl.gov (C.R. Yonker).

0022-328X/02/$ - see front matter
PII: S0022-328X(02)01217-2

sapphire NMR vessel to investigate the hydroformylation of hexene in supercritical CO_2. Other experimental efforts in supercritical fluids have used NMR as an off-line monitor for batch reaction processes, [14,17] or used high-pressure NMR to study hydroformylation reactions in liquid hydrocarbon solvents [20–24].

The experimental effort reported here details the hydroformylation reaction of ethylene using the (p-$CF_3C_6H_4)_3P$ ligand with the rhodium catalyst precursor $Rh(CO)_2$acac in liquid CO_2 at 10 and 23 °C. The subsequent reactions of $HRh(CO)((p\text{-}CF_3C_6H_4)_3P)_3$ during hydroformylation were investigated by high-pressure NMR in a stepwise manner, first C_2H_4 (12.5 bar) was mixed with CO_2 and secondly, a small amount of C_2H_4 (3 bar) in an excess of H_2–CO was mixed with CO_2 in an attempt to characterize the complexes formed during the reaction. Further investigations of the fundamental physicochemical behavior of Rh catalysts and hydroformylation reactions in sub- and supercritical fluids are needed for the development of commercial processes based on these solvents.

2. Experimental

The gases H_2–CO (1:1), ethylene (99.99%), and CO_2 (SFC Grade) were purchased from Scott Specialty Gases and used without further purification. The compounds $Rh(CO)_2$acac and (p-$CF_3C_6H_4)_3P$ were purchased from Strem and used as received. All spectra were acquired on a Varian (VXR-300) 300 MHz pulsed NMR spectrometer with a 7.04 T superconducting magnet and chemical shifts (δ) are reported in ppm. The ^{1}H-NMR spectra are externally referenced to Me_4Si and the ^{31}P-NMR spectra to phosphoric acid. Pressure was measured using a strain gauge with a precision of ±10 psi. Temperature was controlled to ±0.1 K using the nitrogen gas bath controller on the NMR spectrometer.

2.1. Construction of the PEEK NMR cell

The polyether ether ketone (PEEK) NMR cell is based on a similar design published by Wallen et al. [25] (Fig. 1). The current PEEK cell design uses a cone and taper high-pressure sealing surface within the cap instead of an o-ring seal. The cap is made from carbon fiber reinforced PEEK and the cell body from PEEK. The dimensions of the cell are 3 mm ID, 10 mm OD, and ~6.5 cm long. Connection to the cap is with a PEEK finger-tight fitting, using PEEK 1/16 in. OD by.01 in. ID tubing for connection to the SS316 gas manifold system connected to an ISCO pump.

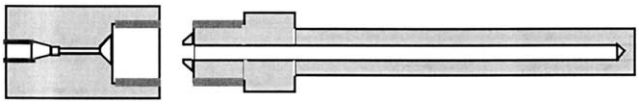

Fig. 1. Schematic of PEEK NMR cell.

2.1.1. Safety considerations

This cell design was hydrostatically tested at room temperature (r.t.) to failure at 1000 bar and beyond with the time for failure being determined. From this information the mean time between failure at 500 bar could be determined. However, unlike metal vessels, it is impossible to specify a maximum working pressure or time limit for the PEEK NMR cell. As with all high-pressure experiments, laboratory personnel should not be directly exposed to the pressurized vessel. Use of the PEEK NMR cell should follow established protocols for length of time exposed to pressure and temperature, and determining the radial dimension for any sign of polymer stress.

2.2. General procedure for the rhodium catalyzed hydroformylation of ethylene in liquid CO_2

In a typical experiment, the PEEK NMR cell was charged with 4.9 mg (19 mmoles) of $Rh(CO)_2$acac and 26.5 mg (57 mmoles) of (p-$CF_3C_6H_4)_3P$ for a ~3:1 mole ratio of ligand to Rh and then evacuated. The maximum concentration in the PEEK NMR cell was ~32 mM for the rhodium catalyst. Next, ~25 bar of H_2–CO (1:1) (300 mmoles of each) was added to the PEEK cell, followed by adjusting the total pressure to 207 bar with CO_2. This solution diffusionally mixed and reacted at 50 °C for ~60 min. Following this time period the sample was cooled, depressurized, and evacuated over night to remove any volatile side products (e.g. acetylacetone). The PEEK NMR cell containing the Rh catalyst was then placed in the 10 mm NMR probe in the magnet, pressurized to 20 bar with H_2–CO (1:1), followed by ethylene to a total pressure of 30 bar. Therefore, the partial pressures of the three gases were approximately equal for this set of conditions. The total pressure in the NMR cell was adjusted to a final pressure of 207 bar with CO_2. The hydroformylation reaction kinetics were followed by ^{1}H-NMR spectra recorded at 10 or 15 min intervals at 10 and 23 °C. The relative number of moles of ethylene, propanal, and H_2 were determined from the integration of the respective NMR signals. Concurrently, $^{31}P\{^1H\}$-NMR spectra were recorded to determine which phosphorus-containing species were present during the reaction. After the hydroformylation reaction was completed, the cell could be evacuated and recharged with the reaction gases. Resting states of the rhodium complex were determined by charging the PEEK NMR cell with only ethylene mixed into CO_2 or a large excess of H_2–CO in CO_2.

3. Results and discussion

The investigation of the rhodium catalyzed hydroformylation reaction in liquid CO_2 allows the further investigation of CO_2 as a reaction medium for catalytic processes. NMR facilitates the investigation of reaction intermediates and can be used to follow the course of reaction as a function of pressure and temperature. The rhodium catalyst precursor, $Rh(CO)_2acac$, and the phosphine ligand, $(p\text{-}CF_3C_6H_4)_3P$, were chosen for study due to their solubility in CO_2 and the ease of forming the rhodium catalyst in situ in the PEEK NMR cell. In this manner the catalyst system can be synthesized in the PEEK cell and either kept under vacuum or dissolved in liquid CO_2 until initiating the hydroformylation reaction.

Scheme 1 shows the reaction steps generally accepted for the hydroformylation reaction of alkenes in liquids and supercritical fluids using a rhodium catalyst. The reaction intermediates III–VII have not been identified experimentally [26]. Not included in Scheme 1, for clarity, are the different stereoisomers of the rhodium species. The ^{1}H-NMR spectrum of the ligand, $(p\text{-}CF_3C_6H_4)_3P$, shows two nonequivalent sets of protons on the benzene ring. The $^{31}P\{^1H\}$-NMR spectrum of the ligand, $(p\text{-}CF_3C_6H_4)_3P$, dissolved in pure CO_2 shows a sharp singlet at ~ -5.0 ppm.

Fig. 2(A) shows the $^{31}P\{^1H\}$-NMR spectrum of $HRh(CO)((p\text{-}CF_3C_6H_4)_3P)_3$, prepared in situ, dissolved in CO_2 at 10.0 °C and 223 bar. The catalyst formation reaction was completed with 20 bar of syngas in CO_2 for ~ 1 h at 50 °C in the PEEK NMR cell. After this time, the NMR cell was evacuated for ~ 24 h to remove any

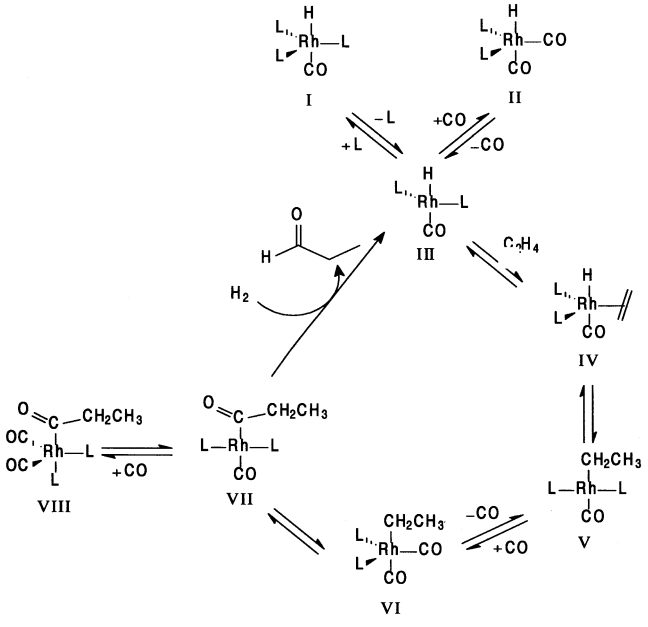

Scheme 1. Accepted mechanism for the hydroformylation of ethylene catalyzed by a Rh(I) complex [26].

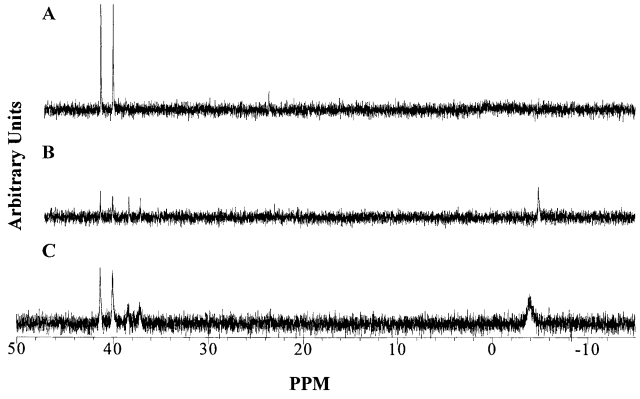

Fig. 2. (A) $^{31}P\{^1H\}$-NMR spectrum, upon removal of the syngas, after reaction of $Rh(CO)_2acac$, $(p\text{-}CF_3C_6H_4)_3P$, and syngas at 10.0 °C and 223 bar in CO_2, (B) $^{31}P\{^1H\}$-NMR spectrum of the reaction between $Rh(CO)_2acac$ and $(p\text{-}CF_3C_6H_4)_3P$ with 10 bar $CO–H_2$ in CO_2 at 22.8 °C and 223 bar total pressure, and (C) $^{31}P\{^1H\}$-NMR spectrum of the reaction between $Rh(CO)_2acac$ and $(p\text{-}CF_3C_6H_4)_3P$ with 10 bar $CO–H_2$ in CO_2 at 40.0 °C and 223 bar total pressure.

volatile products, then the precipitated solid was redissolved in CO_2 at 10.0 °C. The only phosphorus-containing species observed under these conditions in the CO_2 solution was $HRh(CO)((p\text{-}CF_3C_6H_4)_3P)_3$. As expected for a 3:1 PR_3:Rh mole ratio, there was no free phosphine ligand present in this solution. The minor peak at ~ 24.0 ppm is due to a small amount of the phoshine oxide, $(p\text{-}CF_3C_6H_4)_3P{=}O$ [27]. Fig. 2(B), is the $^{31}P\{^1H\}$-NMR spectrum of both $HRh(CO)((p\text{-}CF_3C_6H_4)_3P)_3$ and $HRh(CO)_2((p\text{-}CF_3C_6H_4)_3P)_2$ formed in situ in the PEEK NMR cell from a mixture of the ligand, $Rh(CO)_2acac$ and $H_2–CO$ dissolved in CO_2 at 22.8 °C and 223 bar total pressure (3:1 PR_3:Rh mole ratio). Fig. 2(C) is the $^{31}P\{^1H\}$-NMR spectrum of both $HRh(CO)((p\text{-}CF_3C_6H_4)_3P)_3$ and $HRh(CO)_2((p\text{-}CF_3C_6H_4)_3P)_2$ formed in situ in the PEEK NMR cell from a mixture of the ligand, $Rh(CO)_2acac$ and $H_2–CO$ dissolved in CO_2 at 40.0 °C and 223 bar total pressure (3:1 PR_3:Rh mole ratio). The free phosphine, $(p\text{-}CF_3C_6H_4)_3P$, can also be seen in Fig. 2(B) and (C) over a chemical shift region of $\delta \sim -3.0$ to -5.5 at these temperatures, consistent with loss of phosphine from the $HRh(CO)((p\text{-}CF_3C_6H_4)_3P)_3$ to form $HRh(CO)_2((p\text{-}CF_3C_6H_4)_3P)_2$. The broadening in the ^{31}P signals in Fig. 2(C) as the temperature increases is due to chemical exchange, similar to that reported by Horvath et al. [28] for the water soluble $HRh(CO)[P(m\text{-}C_6H_4SO_3Na)_3]_3$ system.

Bianchini et al. [20] reports for $HRh(CO)(PPh_3)_3$ a doublet centered at δ 41.3 (toluene-d_8) in the $^{31}P\{^1H\}$-NMR spectrum with a one-bond rhodium–phosphorous coupling constant of 153.9 Hz. On pressurizing the solution with $H_2–CO$ at room temperature, the authors report the formation of several products which includes the carbonylation of $HRh(CO)(PPh_3)_3$ to $HRh(CO)_2(PPh_3)_2$. The $^{31}P\{^1H\}$-NMR spectrum (tolu-

ene-d_8) has a signal at δ 37.8 (d, $^1J_{P-Rh} = 138.7$ Hz), which is assigned as the $HRh(CO)_2(PPh_3)_2$ complex, and a signal at δ −4.8 (s), which corresponds to free PPh_3. For $HRh(CO)((p\text{-}CF_3C_6H_4)_3P)_3$, Palo and Erkey [17] report a doublet centered at δ 40.2 ($^1J_{P-Rh} = 156$ Hz) and a signal for the free ligand at δ −6.3 in the $^{31}P\{^1H\}$-NMR spectrum ($CDCl_3$). Based on the NMR data described above in toluene-d_8 and $CDCl_3$ for the $HRh(CO)_2(PPh_3)_2$ and $HRh(CO)((p\text{-}CF_3C_6H_4)_3P)_3$ complexes, the doublet at δ 40.5 ($^1J_{P-Rh} = 156$ Hz) in Fig. 2 is assigned as $HRh(CO)((p\text{-}CF_3C_6H_4)_3P)_3$ and the doublet at δ 37.6 ($^1J_{P-Rh} = 145$ Hz) in Fig. 2(B) and (C) is assigned as $HRh(CO)_2((p\text{-}CF_3C_6H_4)_3P)_2$. Table 1 lists the $^{31}P\{^1H\}$-NMR chemical shift values and the one-bond phosphorus–rhodium coupling constants for these complexes and other structures shown in Scheme 1 observed in situ in liquid CO_2.

Our observations are in contrast to Horvath's work in toluene-d_8 and Leitner's work in $scCO_2$ [19,28]. We see both species, $HRh(CO)((p\text{-}CF_3C_6H_4)_3P)_3$ and $HRh(CO)_2((p\text{-}CF_3C_6H_4)_3P)_2$ present in CO_2 with syngas, whereas Horvath only reports $HRh(CO)_2((p\text{-}CF_3C_6H_4)_3P)_2$ after $HRh(CO)((p\text{-}CF_3C_6H_4)_3P)_3$ is exposed to syngas and Leitner reports only $HRh(CO)_2(3\text{-}H^2F^6\text{-}(R,S)\text{-BINAPHOS})_2$ in $scCO_2$. In fact, ours is the first observation of a significant amount of the monocarbonyl rhodium monomer, $HRh(CO)((p\text{-}CF_3C_6H_4)_3P)_3$ observed in situ under syngas. We believe these differences may be due to solvent effects. In all previous cases, the in situ spectroscopic study was performed in the presence of a hydrocarbon solvent while CO_2 appears to yield a different ratio of the organometallic products. In addition, Leitner's observations were carried out in the presence of a small amount of THF and with a bidendate ligand in which the chelating binding mode is the most stable. We do not observe in the NMR spectra the Rh(0) dimers at these temperatures (10 °C and 23 °C), $Rh_2(\mu\text{-}CO)_2(CO)_{2+x}((p\text{-}CF_3C_6H_4)_3P)_{4-x}$ ($x = 0$, 1, or 2), reported by Bianchini et al. [20] at −20 °C with the PPh_3 ligand using $^{31}P\{^1H\}$-NMR, and by others using high pressure IR in hydrocarbon solvents. We conducted in situ IR studies under identical conditions to our NMR investigations to examine this discrepancy. We found that a yellow precipitate formed, and the FT-IR (Nujol) of the solid is consistent with a Rh(0) dimer, of the form $Rh_2(\mu\text{-}CO)_2(CO)_{2+x}((p\text{-}CF_3C_6H_4)_3P)_{4-x}$ ($x = 0$, 1, or 2). Visual inspection for the Rh(0) dimer in the PEEK NMR cell was not possible.

After the in situ formation of the rhodium catalyst, the high pressure NMR cell was evacuated and the solid precipitate was re-dissolved in CO_2 at 10 °C and 223 bar. In CO_2, with no syngas present, the sole rhodium containing species should be $HRh(CO)((p\text{-}CF_3C_6H_4)_3P)_3$. The ^1H-NMR spectrum of the hydride region of $HRh(CO)((p\text{-}CF_3C_6H_4)_3P)_3$ is shown in Fig. 3. The hydride proton of $HRh(CO)((p\text{-}CF_3C_6H_4)_3P)_3$ appears as a quartet, which is centered at δ −10.2 (see Table 1). The ^1H spectrum shown in Fig. 3 was obtained under the same conditions as Fig. 2(A), with no syngas present in the sample. The one-bond rhodium–proton coupling constant could not be resolved. The two-bond phosphorous–proton coupling constant of ~14 Hz is consistent with a hydride in the apical position *cis* to the three equatorial phosphines in a trigonal bipyramidal geometry [29].

In the CO_2 solution with syngas present, the signal in the ^1H-NMR for the hydrides corresponding to structures I and II (see Scheme 1) observed at 10 °C and 23 °C were extremely broad due to chemical exchange. This made it difficult to directly identify the hydride of $HRh(CO)_2((p\text{-}CF_3C_6H_4)_3P)_2$ from the ^1H spectrum.

Fig. 4(A) shows the ^1H-NMR spectrum of $HRh(CO)((p\text{-}CF_3C_6H_4)_3P)_3$ after exposure to 12.5 bar of ethylene in 207 bar CO_2 at 0 °C. The ethylene (δ ~ 5.5) and ligand (δ 7–8) signals are not shown for clarity. The two signals at chemical shifts of 2 ppm and ~1.4 ppm are unbound acetylacetone from the Rh precursor molecule. The signal at ~0.9 ppm in Fig. 4(A) could be due to ethylene bound to rhodium, such as in structure IV in Scheme 1. The solubility of the proposed ethylene complex, $HRh(CO)((p\text{-}CF_3C_6H_4)_3P)_2(\eta^2\text{-}C_2H_4)$, appears to be greater than $HRh(CO)((p\text{-}CF_3C_6H_4)_3P)_3$ in pure CO_2 at 0 °C. The extreme upfield shift (0.9 ppm) for the signal corresponding to the bound ethylene of $HRh(CO)((p\text{-}CF_3C_6H_4)_3P)_2(\eta^2\text{-}C_2H_4)$ is similar to our

Table 1
Properties of the different rhodium complexes with the $(p\text{-}CF_3C_6H_4)_3P$ ligand as determined by high-pressure NMR

Complex structure [a]	Free ligand $^{31}P\{^1H\}$-NMR (ppm)	Rh complexes $^{31}P\{^1H\}$-NMR (ppm, d)	$^1J_{P-Rh}$ (Hz)	Rh complexes, hydride signal ^1H-NMR (ppm)
I	−5.06	40.5	~156	−10.2
I [b]	−6.3	40.2	156	−9.9
II	−5.06	37.6	~145	
IV		36.5	~197	
VIII		32.0	~82	

[a] Structures are shown in Scheme 1.
[b] From ref [17] in $CDCl_3$.

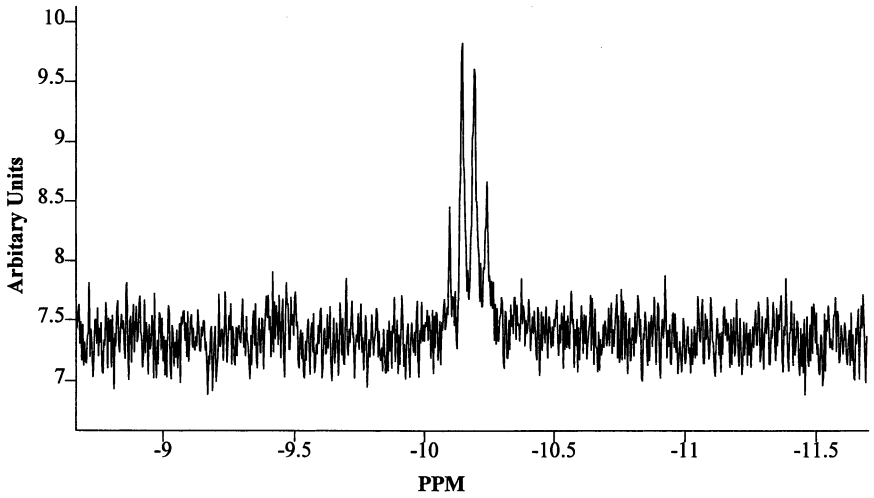

Fig. 3. ^{1}H-NMR spectrum, upon removal of the syngas, after reaction of $Rh(CO)_2acac$, $(p\text{-}CF_3C_6H_4)_3P$, and syngas at 10.0 °C and 223 bar in CO_2.

earlier high-pressure NMR photolysis work using $MeCpMn(CO)_2(\eta^2\text{-}C_2H_4)$ and $CpRe(CO)_2(\eta^2\text{-}C_2H_4)$ in supercritical ethylene and CO_2–C_2H_4 mixtures [30,31]. In these cases, the $\eta^2\text{-}C_2H_4$ was reported at ~2.5 ppm for $MeCpMn(CO)_2(\eta^2\text{-}C_2H_4)$ in ethylene at 0 °C and 274 bar, and at 2.07 ppm for the photolysis product $CpRe(CO)_2(\eta^2\text{-}C_2H_4)$ in liquid C_6D_6. The ^{1}H chemical shifts are density (pressure) dependent. We have observed pressure dependent ^{1}H chemical shift changes greater than 1 ppm [30]. Therefore, the assignment of the peak at ~0.9 ppm to the $\eta^2\text{-}C_2H_4$ adduct is plausible. The molecular symmetry change on the addition of the ethylene to the rhodium complex was observed in the hydride splitting of $HRh(CO)((p\text{-}CF_3C_6H_4)_3P)_2(\eta^2\text{-}C_2H_4)$. The quartet shown in Fig. 3 for $HRh(CO)((p\text{-}CF_3C_6H_4)_3P)_3$ becomes a multiplet of either a triplet or a doublet of doublets. Further investigations are necessary to confirm the structure of the species assigned as the ethylene complex. In a similar manner, the $^{31}P\{^{1}H\}$-NMR spectrum of the proposed $HRh(CO)((p\text{-}CF_3C_6H_4)_3P)_2(\eta^2\text{-}C_2H_4)$ product shows a different one-bond phosphorus–rhodium coupling constant compared with $HRh(CO)((p\text{-}CF_3C_6H_4)_3P)_3$. Fig. 5 shows the in situ $^{31}P\{^{1}H\}$-NMR spectrum of the reaction mixture under the same conditions as shown in Fig. 4. The doublet at ~36.5 ppm ($^{1}J_{P-Rh} = 197$ Hz) is assigned to the $HRh(CO)((p\text{-}CF_3C_6H_4)_3P)_2(\eta^2\text{-}C_2H_4)$ complex (see Table 1). The doublet centered at 40.5 ppm ($^{1}J_{P-Rh} = 155$ Hz) corresponds to $HRh(CO)((p\text{-}CF_3C_6H_4)_3P)_3$.

The acyl complexes (structures VII and VIII in Scheme 1) were investigated by exposing $HRh(CO)((p\text{-}CF_3C_6H_4)_3P)_3$ to an excess amount of H_2–CO (1:1) in the presence of a small partial pressure of ethylene. The

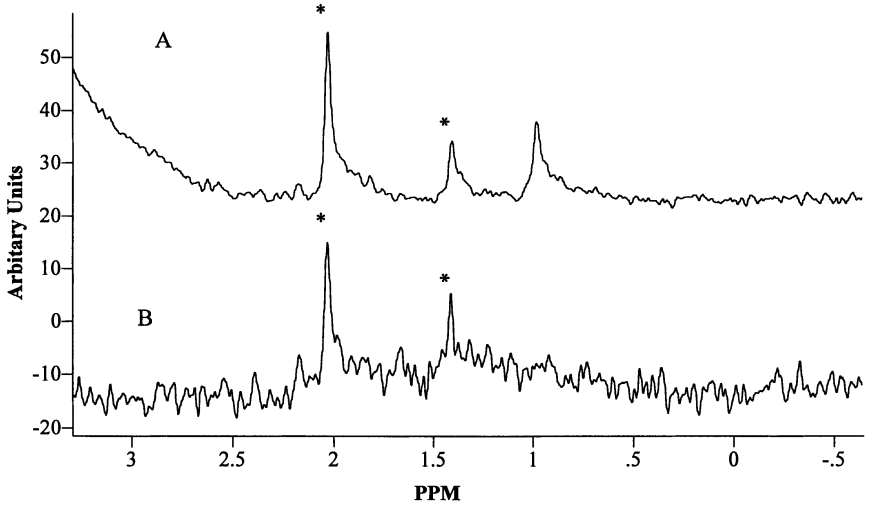

Fig. 4. (A) ^{1}H-NMR spectrum of $HRh(CO)((p\text{-}CF_3C_6H_4)_3P)_3$ and ethylene (12.5 bar) in CO_2 at 207 bar and 0 °C and (B) ^{1}H-NMR spectrum of $HRh(CO)((p\text{-}CF_3C_6H_4)_3P)_3$ in CO_2 at 207 bar and 0 °C, before exposure to ethylene. The peaks labeled by * are due to the enol form of acetylacetone from the Rh precursor molecule.

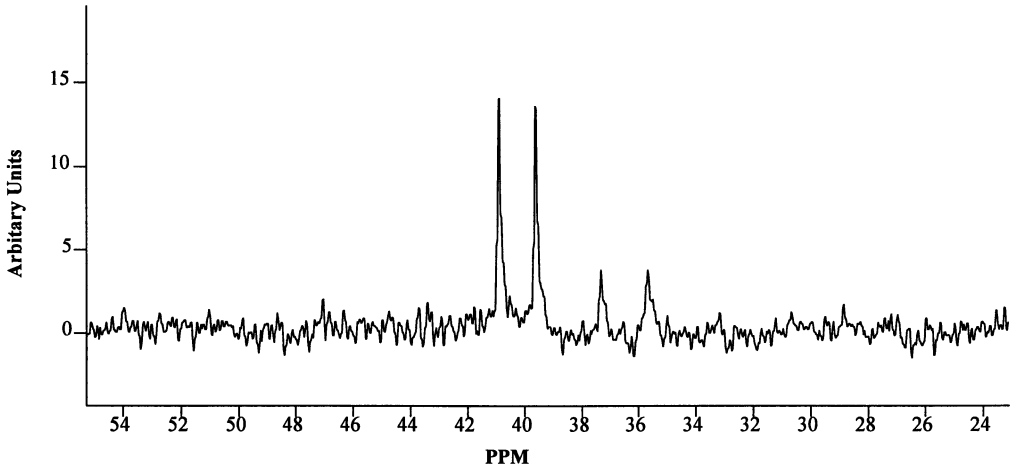

Fig. 5. $^{31}P\{^{1}H\}$-NMR spectrum of a mixture containing $HRh(CO)((p\text{-}CF_3C_6H_4)_3P)_2(\eta^2\text{-}C_2H_4)$ and $HRh(CO)((p\text{-}CF_3C_6H_4)_3P)_3$ in CO_2 at 0 °C and 207 bar. This spectrum was obtained after exposure of $HRh(CO)((p\text{-}CF_3C_6H_4)_3P)_3$ to ~10 bar of ethylene.

resulting $^{31}P\{^{1}H\}$-NMR spectrum of such an experiment is shown in Fig. 6. In this experiment, $HRh(CO)((p\text{-}CF_3C_6H_4)_3P)_3$ was exposed to 3 bar of ethylene and ~138 bar of H_2–CO (1:1) in a total final pressure of 207 bar in CO_2. The H_2–CO (1:1) gas mixture acted as an anti-solvent for the Rh complex causing precipitation. Therefore, the sample mixture in the PEEK NMR cell was evacuated to ~20 bar and then re-pressurized with CO_2 to a final pressure of 207 bar. In this manner, the Rh complexes demonstrate enough solubility to be observed by $^{31}P\{^{1}H\}$-NMR.

In Fig. 6(A), the doublet centered at δ 40 is due to $HRh(CO)((p\text{-}CF_3C_6H_4)_3P)_3$ ($^{1}J_{P-Rh} = 155$ Hz). The large singlet signal at δ 32.1 is postulated to be a degradation product of the $(p\text{-}CF_3C_6H_4)_3P$ as it no longer shows coupling to rhodium. Various mechanisms of catalyst deactivation through the degradation of the phosphorus ligand have been proposed [32]. The structure of this degradation product remains to be elucidated. It is unlikely that the degradation product is the phosphine oxide, which appears at ~21 ppm in C_6D_6 in the $^{31}P\{^{1}H\}$-NMR spectrum. The signal at δ 31.5 is actually a doublet with part of the signal being obscured by the much larger signal at 32.1 ppm [33]. The one-bond phosphorus-rhodium coupling constant for this doublet is 82 ± 4 Hz. In the hydroformylation of 1-hexene in toluene-d_8 reported by Bianchini et al., [20] a signal in the $^{31}P\{^{1}H\}$-NMR spectrum at 27.5 ppm (d, $^{1}J_{P-Rh} = 78.0$ Hz) was assigned as the acyl–Rh complex $Rh(CO(CH_2)_5CH_3)(CO)_2(PPh_3)_2$. Considering the different phosphorus ligand and solvent system for the experiment shown in Fig. 6, and the similar one-bond phosphorus–rhodium coupling constant, the signal at 31.5 ppm (d, $^{1}J_{P-Rh} = 82$ Hz) in Fig. 6(A) is most likely due to the acyl–Rh complex shown as structure VIII in Scheme 1 (see Table 1). The PEEK NMR cell containing

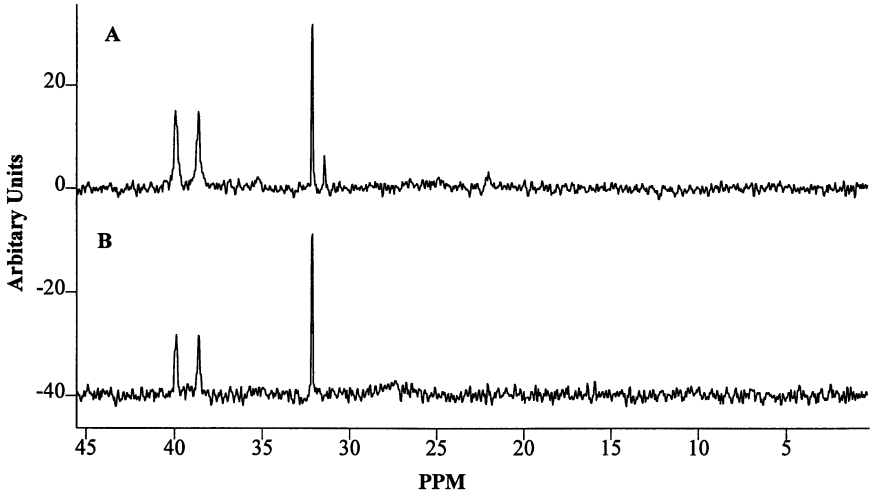

Fig. 6. (A) $^{31}P\{^{1}H\}$-NMR spectrum of the acyl–Rh complex after exposure to 3 bar ethylene, ~138 bar H_2–CO (1:1), and 66 bar CO_2 for 10 min, then depressurized and repressurized to 207bar CO_2 at 50 °C. (B) $^{31}P\{^{1}H\}$-NMR spectrum of the remaining products from the reaction described above after evacuation for 12 h (in CO_2 at 207 bar and 50 °C).

the Rh complex mixture was depressurized and evacuated for ~12 h. On re-pressurizing with CO_2 to a pressure of 207 bar, the spectrum in Fig. 6(B) was obtained, in which the proposed acyl–Rh complex is no longer observed in the system (because of the residual acetylacetone interference, the ^{1}H-NMR was not useful for spectral interpretation of the acyl complex).

The potential application of high-pressure NMR to the hydroformylation reaction of ethylene with a Rh catalyst in CO_2 not only lies with the identification of potential intermediate complexes, but the kinetics of the reaction process can be directly followed through time-resolved NMR acquisition during the reaction. In the temperature range of 10 and 23 °C, the hydroformylation kinetics are slow enough such that the product formation can be followed by recording the NMR spectra. The equation governing the global reaction rate could be determined from a detailed series of experiments covering a range of substrate and reactant concentrations as published previously for CO_2 in a batch reaction process [15–17]. The experiments detailed in the following section are a subset of a wider range of experimental conditions proposed for investigation at a future date. The rate of the hydroformylation reaction of ethylene in CO_2 with a rhodium catalyst was determined by measuring the peak areas of the reactants (ethylene and H_2) and the product (propanal) in the ^{1}H-NMR spectrum as a function of time.

A typical experimental result is shown in Fig. 7. The spectrum is a snapshot of the hydroformylation reaction 140 min after the initiation of the reaction. The experimental mole ratio of ligand:Rh is 3:1, the mole ratio of C_2H_4:Rh is ~18:1, with 20 bar of H_2–CO (1:1), and an ethylene pressure of 10 bar in CO_2 at a total final pressure of 207 bar and 10 °C. As can be seen in Fig. 7, the different species in solution are identified and the area of the signals can be determined.

For the two temperatures of 10 and 23 °C, the peak areas were normalized by the number of protons giving rise to the resonance signal. The normalized peak area, which is proportional to the number of moles, can then be plotted for the hydroformylation reaction as a function of time. These data are plotted in Fig. 8, for the conditions of 3:1 ligand:Rh mole ratio and approximately equal pressures for the three gases (ethylene, H_2 and CO) of ~12.5 bar at the two temperatures. At both 10 and 23 °C, the propanal formation is linear as a function of time. This relationship allows the turn-over frequency for the formation of the aldehyde ([mol aldehyde][mol Rh]$^{-1}$ h^{-1}) to be determined for these two temperatures over a large reaction time. These observed frequencies are ~5 [mol aldehyde][mol Rh]$^{-1}$ h^{-1} and ~34 [mol aldehyde][mol Rh]$^{-1}$ h^{-1} at 10 and 23 °C, respectively. The catalyst species present during the hydroformylation reaction were monitored by ^{31}P{^{1}H}-NMR, only structures I and II were seen in equilibrium in solution with a small amount of oxidized ligand present at longer times.

4. Conclusions

In situ high-pressure NMR investigations of homogenous catalytic reactions in liquid and supercritical CO_2 are useful in identifying reaction intermediates and determining observed reaction rates. The investigation of the rhodium catalyzed hydroformylation reaction of ethylene in liquid CO_2 demonstrates the advantages of such a spectroscopic investigation. The proposed HRhCO((*p*-$CF_3C_6H_4$)$_3$P)$_2$(η^2-C_2H_4) intermediate was identified directly in situ for the first time. This preliminary set of experiments demonstrates that high-pressure NMR can be used to observe in situ the reaction in supercritical CO_2 solvent between highly

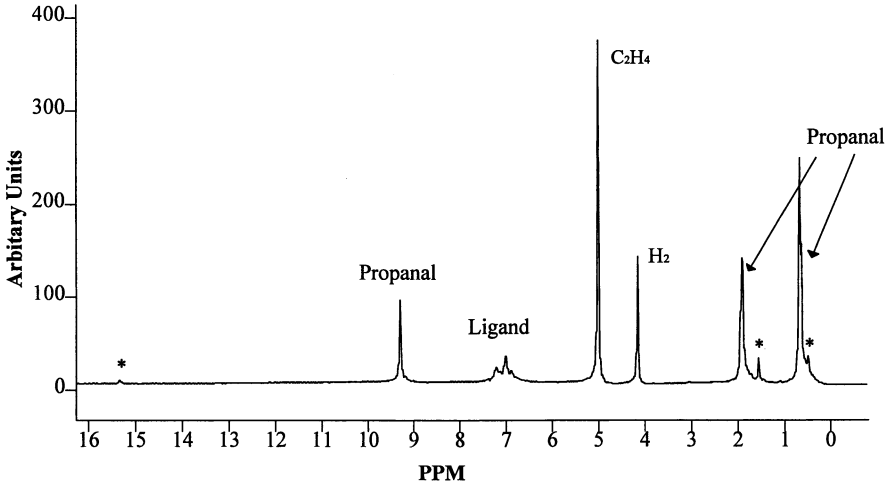

Fig. 7. ^{1}H-NMR spectrum during the hydroformylation reaction of ethylene after 140 min. Reaction conditions are 3:1 ligand:Rh mole ratio, 20 bar H_2–CO (1:1), 10 bar ethylene, final pressure 207 bar CO_2 at 10 °C. The peaks labeled by * are due to acetylacetone from the Rh precursor molecule.

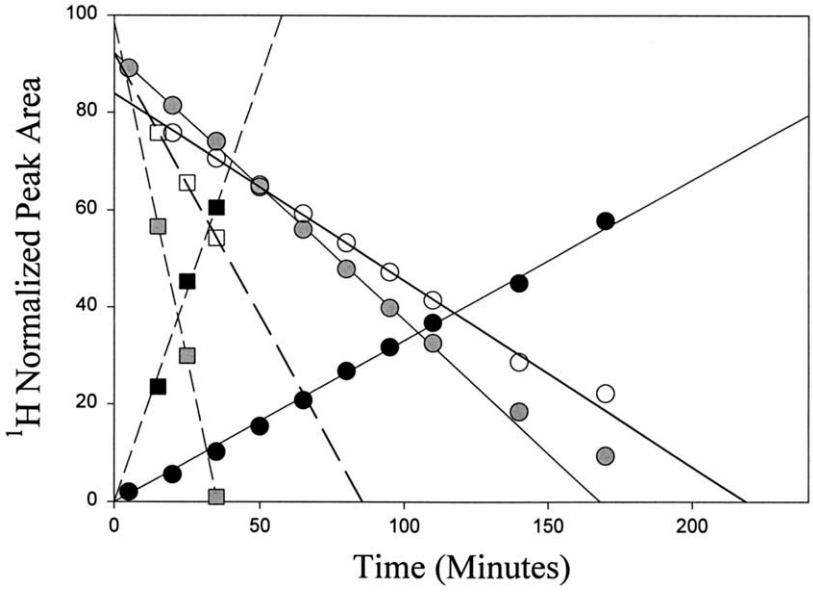

Fig. 8. Normalized peak area versus reaction time for the ^{1}H-NMR spectra during the hydroformylation reaction. Ethylene (○, □), H_2 (●, ■) and Propanal (●, ■) are shown at 10 °C (circle symbols, solid lines) and 23 °C (square symbols, dashed lines).

soluble gaseous reactants and an organometallic catalyst. This technique is useful for determining reaction intermediates and describing the turn-over frequency of reactions in sub- and supercritical fluids. A more detailed investigation of the hydroformylation system reported here is in progress. It is expected that as supercritical fluids extend themselves into the realm of reaction solvents for large-scale or commercial processes, further effort will be needed to identify the fundamental reaction mechanism under such solvent conditions.

Acknowledgements

The authors would like to thank Dr. A. Getty for her helpful comments regarding this manuscript. Work at the Pacific Northwest National Laboratory (PNNL) was supported by the Office of Science, Office of Basic Energy Sciences, Chemical Sciences Division of the US Department of Energy, under Contract DE-AC076RLO 1830.

References

[1] P.G. Jessop, Y. Hsiao, T. Ikariya, R. Noyori, J. Am. Chem. Soc. 118 (1996) 344.
[2] P.G. Jessop, T. Ikariya, R. Noyori, Organometallics 14 (1995) 1510.
[3] P.G. Jessop, T. Ikariya, R. Noyori, Science 269 (1995) 1065.
[4] M.J. Burk, S. Feng, M.F. Gross, W. Tumas, J. Am. Chem. Soc. 117 (1995) 8278.
[5] P.G. Jessop, T. Ikariya, R. Noyori, Nature 368 (1994) 231.
[6] D.K. Morita, D.R. Pesiri, S.A. David, W.H. Glaze, W. Tumas, Chem. Commun. (1998) 1397.
[7] M.A. Carroll, A.B. Holmes, Chem. Commun. (1998) 1395.
[8] J.W. Rathke, R.J. Klinger, United States Patent, 5,198,589,1993.
[9] J.W. Rathke, R.J. Klinger, T.R. Krause, Organometallics 11 (1992) 585.
[10] J.W. Rathke, R.J. Klinger, T.R. Krause, Organometallics 10 (1991) 1350.
[11] Y. Guo, A. Akgerman, Ind. Eng. Chem. Res. 36 (1997) 4581.
[12] Y. Guo, A. Akgerman, J. Supercrit. Fluids 15 (1999) 63.
[13] S. Kainz, D. Koch, W. Baumann, W. Leitner, Angew. Chem. Int. Ed. Engl. 36 (1997) 1628.
[14] D. Koch, W. Leitner, J. Am. Chem. Soc. 120 (1998) 13398.
[15] D.R. Palo, C. Erkey, Ind. Eng. Chem. Res. 37 (1998) 4203.
[16] D.R. Palo, C. Erkey, Ind. Eng. Chem. Res. 38 (1999) 3786.
[17] D.R. Palo, C. Erkey, Organometallics 19 (2000) 81.
[18] A. Fürstner, D. Koch, K. Langemann, W. Leitner, C. Six, Angew. Chem. Int. Ed. Engl. 36 (1997) 2466.
[19] G. Francio, K. Wittmann, W. Leitner, J. Organomet. Chem. 621 (2001) 130.
[20] C. Bianchini, H.M. Lee, A. Meli, F. Vizza, Organometallics 19 (2000) 849.
[21] C. Bianchini, P. Barbaro, G. Scapacci, F. Zanobini, Organometallics 19 (2000) 2450.
[22] S.C. van der Slot, P.C.J. Kamer, P.W.N.M. van Leeuwen, J.A. Iggo, B.T. Heaton, Organometallics 20 (2001) 430.
[23] F.R. Bergman, J.M. Ernsting, F. Müller, M.D.K. Boele, L.A. van der Veen, C.J. Elesevier, J. Organomet. Chem. 592 (1999) 306.
[24] A. Castellanos-Páez, S. Castillón, C. Claver, P.W.N.M. van Leeuwen, W.G.J. de Lange, Organometallics 17 (1998) 2543.
[25] S.L. Wallen, L.K. Schoenbachler, E.D. Dawson, M.A. Blatchford, Anal. Chem. 72 (2000) 4230.
[26] P.W.N.M. van Leeuwen, C.P. Casey, G.T. Whiteker, in: P.W.N.M. van Leuwen, C. Claver (Eds.), Rhodium Catalyzed Hydroformylation Chapter 4, Kluwer Academic Publishers, Dordrecht, 2000, p. 64.
[27] The $(p\text{-}CF_3C_6H_4)_3P$ phosphine was oxidized by the reaction with excess t-butylperoxide in benzene. Gentle heating was necessary to complete the reaction. The product was observed by ^{31}P-NMR.

[28] I.T. Horvath, R.V. Kastrup, A.A. Oswald, E.J. Mozeleski, Catal. Lett. 2 (1989) 85.
[29] L.A. van der Veen, M.D.K. Boele, F.R. Bregman, P.C.J. Kramer, P.W.N.M. van Leeuwen, K. Goubitz, J. Fraanje, H. Schenk, C. Bo, J. Am. Chem. Soc. 120 (1998) 11616.
[30] J.C. Linehan, S.L. Wallen, C.R. Yonker, T.E. Bitterwolf, J.T. Bays, J. Am. Chem. Soc. 119 (1997) 10170.
[31] J.C. Linehan, C.R. Yonker, J.T. Bays, S.T. Autrey, T.E. Bitterwolf, S. Gallagher, J. Am. Chem. Soc. 120 (1998) 5826.
[32] A.M. Trzeciak, J.J. Ziólkowski, Coord. Chem. Rev. 190–192 (1999) 883.
[33] On expansion of this region of the $^{31}P\{^{1}H\}$-NMR spectrum, the second peak of the doublet can be discerned on the shoulder of the larger peak at 32.1 ppm.